

# On Covering a Solid Sphere with Concentric Spheres in $\mathbb{Z}^3$ <sup>☆</sup>

Sahadev Bera<sup>a</sup>, Partha Bhowmick<sup>b,\*</sup>, Bhargab B. Bhattacharya<sup>a</sup>

<sup>a</sup>Advanced Computing and Microelectronics Unit, Indian Statistical Institute, Kolkata, India

<sup>b</sup>Computer Science and Engineering Department, Indian Institute Technology, Kharagpur, India

September 05, 2014

---

## Abstract

We show that a digital sphere, constructed by the circular sweep of a digital semicircle (generatrix) around its diameter, consists of some holes (absentee-voxels), which appear on its spherical surface of revolution. This incompleteness calls for a proper characterization of the absentee-voxels whose restoration will yield a complete spherical surface without any holes. In this paper, we present a characterization of such absentee-voxels using certain techniques of digital geometry and show that their count varies quadratically with the radius of the semicircular generatrix. Next, we design an algorithm to fill these absentee-voxels so as to generate a spherical surface of revolution, which is more realistic from the viewpoint of visual perception. We further show that covering a solid sphere by a set of complete spheres also results in an asymptotically larger count of absentees, which is cubic in the radius of the sphere. The characterization and generation of complete solid spheres without any holes can also be accomplished in a similar fashion. We furnish test results to substantiate our theoretical findings.

**Keywords:** Digital circle, Digital disc, Digital geometry, Geometry of numbers, Image analysis, Number theory

---

## 1. Introduction

Over the last two decades, the studies on geometric primitives in 2D and 3D digital space have gained much momentum because of their numerous applications in computer graphics, image processing, and computer vision. Apart from the characterization of straight lines and planes [7, 9, 10, 17, 18, 23, 28, 32, 48], several theoretical work, mostly on digital spheres and hyperspheres, have appeared in the literature. A majority of them in 3D digital space are based on the extension of similar investigations on the characterization and generation of circles, rings, discs, and circular arcs in the 2D digital plane [1, 2, 16, 19, 20, 29, 41, 43, 45, 49]. For various problems in science and engineering, discrete spheres are often required for simulation of experiments. For example, in [21, 50], discrete spheres are used to test the accuracy of the *discrete dipole approximation* (DDA)

---

<sup>☆</sup>A preliminary version of this work has appeared in ICAA'14 [3].

\*Author for correspondence.

*Email addresses:* sahadevbera@gmail.com (Sahadev Bera), pb@cse.iitkgp.ernet.in, bhowmick@gmail.com (Partha Bhowmick), bhargab@isical.ac.in (Bhargab B. Bhattacharya)

for computing scattering and absorption by isolated, homogeneous spheres, as well as by targets consisting of two contiguous spheres. Hence, with the emergence of new paradigms, such as digital calculus [42], digital geometry [33], theory of words and numbers [34, 39], an appropriate characterization of a digital sphere is required to enrich our understanding of objects in 3D discrete space.

In this work, we address the problem of constructing a *closed digital surface* defined by a set of points in  $\mathbb{Z}^3$  such that they optimally approximate a real sphere with integer radius. Some prior work closely resemble our work, but they deal with spheres with a real value of radius. For example, there is a multitude of papers in the literature, which discuss how to find the lattice points on or inside a real sphere of a given radius [8, 30, 14, 13, 27, 38, 22, 47]. Some of them addresses the problem of finding a real sphere that passes through a given set of lattice points [37]. They are closely related to the determination of lattice points on circles [11, 31], ellipsoids [15, 35], or on several types of surfaces of revolution [12].

For hypersphere generation, characterization of a discrete analytical hypersphere has been done in [2] to develop an algorithm, which is an extension of the algorithm for generating discrete analytical circles. The algorithm is, however, quite expensive owing to complex operations in the real space. An extension of the idea used in [2] has been done in [24] based on a non-constant thickness function [25], but no algorithm for generation of a digital sphere or hypersphere has been proposed. Recently, analytical descriptions of various classes of digital circles, spheres, and some cases of hyperspheres in a morphological framework have been proposed in [46]. Very recently, the notion of *discrete spherical geodesic path* between two voxels lying on a discrete sphere has been introduced in [6], and a number-theoretic algorithm has been proposed for construction of such paths in optimal time.

In [40], an algorithm for digitization of a real sphere with integer radius has been proposed. It constructs the sphere as a sequence of contiguous digital circles by using Bresenham’s circle drawing algorithm. Such an approach fails to ensure the completeness of the generated digital sphere, since it gives rise to absentee (missing) voxels, as shown in this paper. The digital sphere generated by our algorithm, on the contrary, does not have any absentee-voxel, since it fixes these absentees based on a digital-geometric characterization.

The work proposed in this paper aims to locate and fill the absentee-voxels (3D points with integer coordinates) on a digital spherical surface of revolution. Covering such a surface by coaxial digital circles (with integer radius and integer center) in  $\mathbb{Z}^3$  cannot produce the desired completeness of the surface owing to absentee-voxels. Interestingly, the occurrence of absentees in such a cover is possibly a lesser fact. The greater fact is that the absentees occur in multitude—an observation that motivates the requirement of their proper characterization, which subsequently aids in designing a proven algorithm to generate a complete spherical surface in  $\mathbb{Z}^3$ .

We have organized the rest of the paper as follows. In Sec. 2, we introduce few definitions and important properties related with digital circles, digital discs, and digital spheres considered in our work. In Sec. 3, we derive the necessary and sufficient condition for a voxel to be an absentee in a sphere of revolution. We also prove that the absentee count while covering a digital sphere of radius  $r$  by coaxial digital circles—generated by the circular sweep of a digitally circular arc of radius  $r$  (digital generatrix)—varies quadratically with  $r$ . In Sec. 3.1, we characterize the absentee family, and use it in Sec. 3.2 for fixing the absentees in our proposed algorithm for generating a

complete (i.e., absentee-free) sphere of revolution. In Sec. 4, we discuss further about the absentees in covering a solid sphere by union of complete spheres. We show here that these absentees are of two kinds: *absentee lines* and *absentee circles*. We derive their characterization in Sec. 4.1. We use this characterization in Sec. 4.2 to show that the absentee counts corresponding to absentee lines and absentee circles are  $\Theta(r^{5/2})$  and  $\Theta(r^3)$  respectively. The algorithm for fixing these absentees while generating a complete solid sphere is given in Sec. 4.3. Finally, in Sec. 5, we present some test results to substantiate our theoretical findings.

## 2. Preliminaries

There exist several definitions of digital circles (and discs, spheres, etc.) in the literature, depending on whether the radius and the center coordinates are real or integer values. Irrespective of these definitions, a digital circle (sphere) is essentially a set of points with integer coordinates, which are called *digital points* or *pixels* (*voxels*) [33]. In this paper, we consider the *grid intersection digitization* [33, 44] of a real circle with integer radius and having center with integer coordinates. Such a digitization produces a digital circle, which can be generated by the well-known *midpoint circle algorithm* or the *Bresenham circle algorithm* [26], and its definition is as follows.

**Definition 1** (Digital circle). *A digital circle with radius  $r \in \mathbb{Z}^+$  and center  $o(0, 0)$  is given by  $\mathcal{C}^{\mathbb{Z}}(r) = \left\{ (i, j) \in \mathbb{Z}^2 : \left| \max(|i|, |j|) - \sqrt{r^2 - (\min(|i|, |j|))^2} \right| < \frac{1}{2} \right\}$ .*

The points in  $\mathcal{C}^{\mathbb{Z}}(r)$  are connected in 8-neighborhood. The points defining its *interior* are connected in 4-neighborhood, and hence separated by  $\mathcal{C}^{\mathbb{Z}}(r)$  from its *exterior* points, which are also connected in 4-neighborhood [33].

All the results in this paper are valid for any non-negative integer radius and any center with integer coordinates. So, for sake of simplicity, henceforth we consider the center as  $o$  and use the notation  $\mathcal{C}^{\mathbb{Z}}(r)$  instead of  $\mathcal{C}^{\mathbb{Z}}(o, r)$ , where  $r \in \mathbb{Z}^+ \cup \{0\}$ . We specify it explicitly when the center is not  $o$ .

A real point or a pixel  $(x, y)$  is said to be lying in Octant 1 if and only if  $0 \leq x \leq y$  (Figure 1(a)). We use the notation  $\mathcal{C}_1^{\mathbb{Z}}(r)$  to denote Octant 1 of  $\mathcal{C}^{\mathbb{Z}}(r)$ , and  $\mathbb{Z}_1^2$  to denote all points in Octant 1 of  $\mathbb{Z}^2$ .

**Definition 2** (Digital disc). *A digital disc of radius  $r$  consists of all digital points in  $\mathcal{C}^{\mathbb{Z}}(r)$  and its interior, and is given by*

$$\mathcal{D}^{\mathbb{Z}}(r) = \left\{ (i, j_c) \in \mathbb{Z}^2 : 0 \leq i \cdot i_c \leq i_c^2 \wedge \left| \max(|i_c|, |j_c|) - \sqrt{r^2 - (\min(|i_c|, |j_c|))^2} \right| < \frac{1}{2} \right\}.$$

Note that in Def. 2, the condition  $0 \leq i \cdot i_c \leq i_c^2$  relates a disc pixel  $(i, j_c)$  to a circle pixel  $(i_c, j_c)$ , as  $0 \leq i_c$  implies  $0 \leq i \leq i_c$  and  $i_c \leq 0$  implies  $i_c \leq i \leq 0$ . If we consider the union of all digital circles centered at  $o$  and radius in  $\{0, 1, 2, \dots, r\}$ , then the resultant set  $\mathcal{D}_{\cup}^{\mathbb{Z}}(r) := \bigcup_{s=1}^r \mathcal{C}^{\mathbb{Z}}(s)$

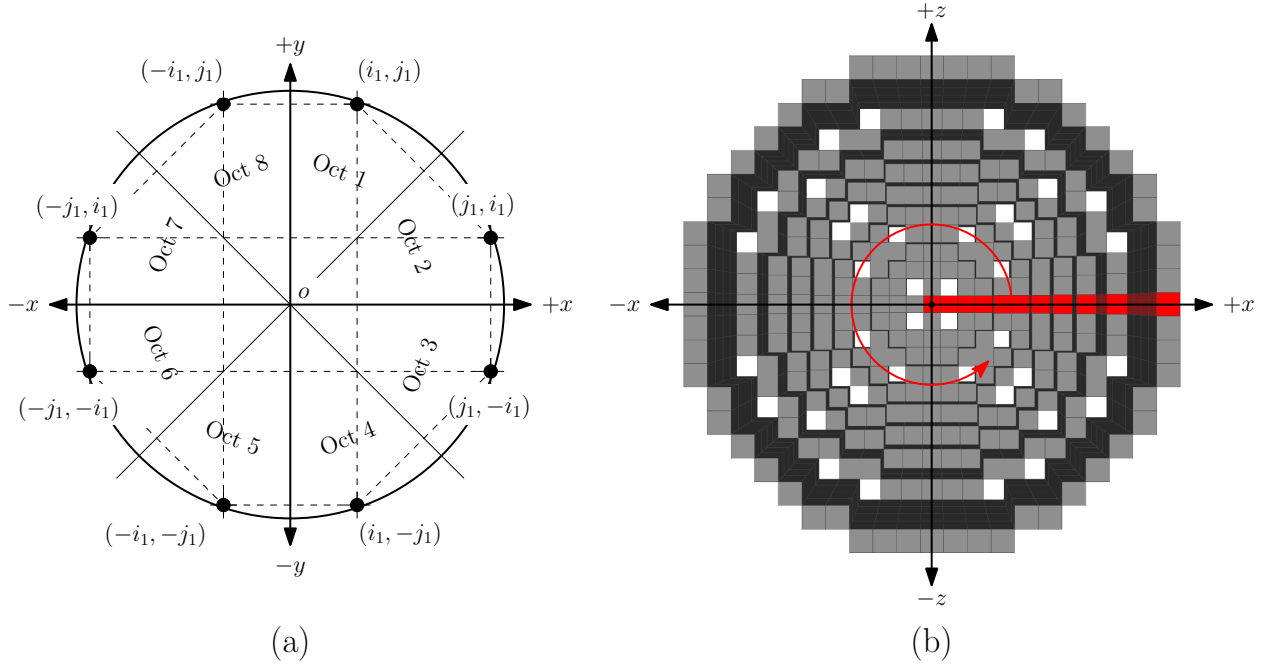


Figure 1: (a) 8-symmetric points  $\{(i, j) : \{|i|\} \cup \{|j|\} = \{i_1, j_1\}\}$  in eight respective octants of a digital circle  $\mathcal{C}^{\mathbb{Z}}(r)$ . (b)  $\mathcal{H}_{\cup}^{\mathbb{Z}}(r)$  for  $r = 10$ , with the  $+y$  axis pointing inwards w.r.t. the plane of the paper.

is not identical with the digital disc of radius  $r$ . The set  $\mathcal{D}_{\cup}^{\mathbb{Z}}(r)$  contains absentee-pixels, as defined below.

**Definition 3** (Disc absentee). *A pixel  $p$  is a disc absentee if and only if there exists some  $r' \in \{1, 2, \dots, r\}$  such that  $p$  is a point in the interior of  $\mathcal{C}^{\mathbb{Z}}(r')$  and in the exterior of  $\mathcal{C}^{\mathbb{Z}}(r' - 1)$ .*

The above definition implies that if  $p$  is any disc absentee, then  $p$  does not belong to any digital circle, i.e.,  $p \in \mathcal{D}^{\mathbb{Z}}(r)$  and  $p \notin \mathcal{D}_{\cup}^{\mathbb{Z}}(r)$ . Hence, the set of disc absentees is given by  $\mathcal{A}^{\mathbb{Z}^2}(r) = \mathcal{D}^{\mathbb{Z}}(r) \setminus \mathcal{D}_{\cup}^{\mathbb{Z}}(r)$ . The above definition of disc absentee is used in the following definitions related to *spherical surfaces of revolution* in  $\mathbb{Z}^3$ . However, henceforth we do not use the term “of revolution” for sake of simplicity. We also drop the term “digital” from any digital surface in  $\mathbb{Z}^3$ .

Let  $\mathcal{C}_{1,2}^{\mathbb{Z}}(r)$  denote the first quadrant (comprising the first and the second octants) of  $\mathcal{C}^{\mathbb{Z}}(r)$ , which is used as the *generatrix*. When we rotate  $\mathcal{C}_{1,2}^{\mathbb{Z}}(r)$  about  $y$ -axis through  $360^\circ$ , we get a stack (sequence) of circles representing a *hemisphere*, namely  $\mathcal{H}_{\cup}^{\mathbb{Z}}(r) := \bigcup_{(i,j) \in \mathcal{C}_{1,2}^{\mathbb{Z}}(r)} \mathcal{C}^{\mathbb{Z}}(c, i)$ , where

$c = (0, j, 0)$  denotes the center of  $\mathcal{C}^{\mathbb{Z}}(c, i)$ , as shown in Figure 1(b). Each circle  $\mathcal{C}^{\mathbb{Z}}(c, i)$  in this stack is generated by rotating a pixel  $(i, j) \in \mathcal{C}_{1,2}^{\mathbb{Z}}(r)$  about  $y$ -axis. The previous circle in the stack is either  $\mathcal{C}^{\mathbb{Z}}(c', i - 1)$  or  $\mathcal{C}^{\mathbb{Z}}(c'', i)$ , where  $c' = (0, j', 0)$  with  $j' \in \{j, j + 1\}$ , and  $c'' = (0, j + 1, 0)$ . There is no absentee between  $\mathcal{C}^{\mathbb{Z}}(c, i)$  and  $\mathcal{C}^{\mathbb{Z}}(c'', i)$ , as they have the same radius. But as the radii of  $\mathcal{C}^{\mathbb{Z}}(c, i)$  and  $\mathcal{C}^{\mathbb{Z}}(c', i - 1)$  differ by unity, there would be absentees (Definition 4) between them in  $\mathcal{H}_{\cup}^{\mathbb{Z}}(r)$ . Each such absentee  $p$  would lie on the plane of  $\mathcal{C}^{\mathbb{Z}}(c, i)$  in the exterior of  $\mathcal{C}^{\mathbb{Z}}(c, i - 1)$ , since  $p$  did not appear in the part of  $\mathcal{H}_{\cup}^{\mathbb{Z}}(r)$  constructed up to  $\mathcal{C}^{\mathbb{Z}}(c', i - 1)$  and appeared only after constructing  $\mathcal{C}^{\mathbb{Z}}(c, i)$ . Hence, we have the following definition.

**Definition 4** (Sphere absentee). *A voxel  $p$  is a sphere absentee lying on the plane  $y = j$  if and only if there exist two consecutive points  $(i, j)$  and  $(i - 1, j')$  in  $\mathcal{C}_{1,2}^{\mathbb{Z}}(r)$ ,  $j' \in \{j, j + 1\}$ , such that  $p$  lies in the interior of  $\mathcal{C}^{\mathbb{Z}}(c, i)$  and in the exterior of  $\mathcal{C}^{\mathbb{Z}}(c, i - 1)$ , where  $c = (0, j, 0)$ .*

On inclusion of the sphere absentees (lying above  $zx$ -plane) with  $\mathcal{H}_{\cup}^{\mathbb{Z}}(r)$ , we get the *complete hemisphere*, namely  $\mathcal{H}^{\mathbb{Z}}(r)$ . On taking  $\mathcal{H}_{\cup}^{\mathbb{Z}}(r)$  and its reflection on  $zx$ -plane, we get the *sphere*, namely  $\mathcal{S}_{\cup}^{\mathbb{Z}}(r)$ . Similarly, the union of  $\mathcal{H}^{\mathbb{Z}}(r)$  and its reflection on  $zx$ -plane gives the *complete sphere* in  $\mathbb{Z}^3$ . Let  $\mathcal{A}^{\mathbb{Z}^3}(r)$  be the set of sphere absentees. The number of points in  $\mathcal{A}^{\mathbb{Z}^3}(r)$  is double the absentee count in  $\mathcal{H}_{\cup}^{\mathbb{Z}}(r)$ . We have the following definitions on spheres and their absentees.

**Definition 5** (Complete sphere). *A complete (hollow) sphere of radius  $r$  is given by  $\mathcal{S}^{\mathbb{Z}}(r) = \mathcal{S}_{\cup}^{\mathbb{Z}}(r) \cup \mathcal{A}^{\mathbb{Z}^3}(r)$ .*

**Definition 6** (Complete solid sphere). *A complete solid sphere  $\mathcal{S}^{\mathbb{Z}}(r)$  of radius  $r$  is given by the union of  $\mathcal{S}^{\mathbb{Z}}(r)$  and voxels lying inside  $\mathcal{S}^{\mathbb{Z}}(r)$ .*

**Definition 7** (Solid sphere absentee). *A voxel  $p$  is a solid sphere absentee if and only if  $p \in \mathcal{S}^{\mathbb{Z}}(r) \setminus \mathcal{S}_{\cup}^{\mathbb{Z}}(r)$ , where  $\mathcal{S}_{\cup}^{\mathbb{Z}}(r) = \bigcup_{r'=0}^r \mathcal{S}^{\mathbb{Z}}(r')$ .*

### 2.1. Previous Results

We need the following results from [4] to count and fix the absentees in the surface of revolution.

**Theorem 1.** *The total count of disc absentees lying in  $\mathcal{D}_{\cup}^{\mathbb{Z}}(r)$  is given by*

$$|\mathcal{A}^{\mathbb{Z}^2}(r)| = 8 \sum_{k=0}^{m_r-1} |\mathcal{A}_k^{\mathbb{Z}^2}(r)|,$$

where  $|\mathcal{A}_k^{\mathbb{Z}^2}(r)| = \left\lceil \sqrt{(2k+1)r - k(k+1)} \right\rceil - \left\lceil 2k+1 + \frac{1}{2}\sqrt{(8k^2+4k+1)} \right\rceil$   
and  $m_r = r - \lceil r/\sqrt{2} \rceil + 1$ .

**Theorem 2.**  $|\mathcal{A}^{\mathbb{Z}^2}(r)| = \Theta(r^2)$ .

### 3. Absentees in a Digital Sphere

As mentioned earlier in Sec. 2, the hemisphere and the sphere have absentee-voxels, which can be characterized based on their unique correspondence with the absentee-pixels of  $\mathcal{D}_{\cup}^{\mathbb{Z}}(r)$ . To establish this correspondence, we consider two consecutive pixels  $p_i(x_i, y_i)$  and  $p_{i+1}(x_{i+1}, y_{i+1})$  of the generating curve  $\mathcal{C}_{1,2}^{\mathbb{Z}}(r)$  corresponding to  $\mathcal{H}_{\cup}^{\mathbb{Z}}(r)$ . We have three possible cases as follows.

1.  $(x_{i+1}, y_{i+1}) = (x_i + 1, y_i)$  (Octant 1)
2.  $(x_{i+1}, y_{i+1}) = (x_i + 1, y_i - 1)$  (Octant 1 or Octant 2)
3.  $(x_{i+1}, y_{i+1}) = (x_i, y_i - 1)$  (Octant 2)

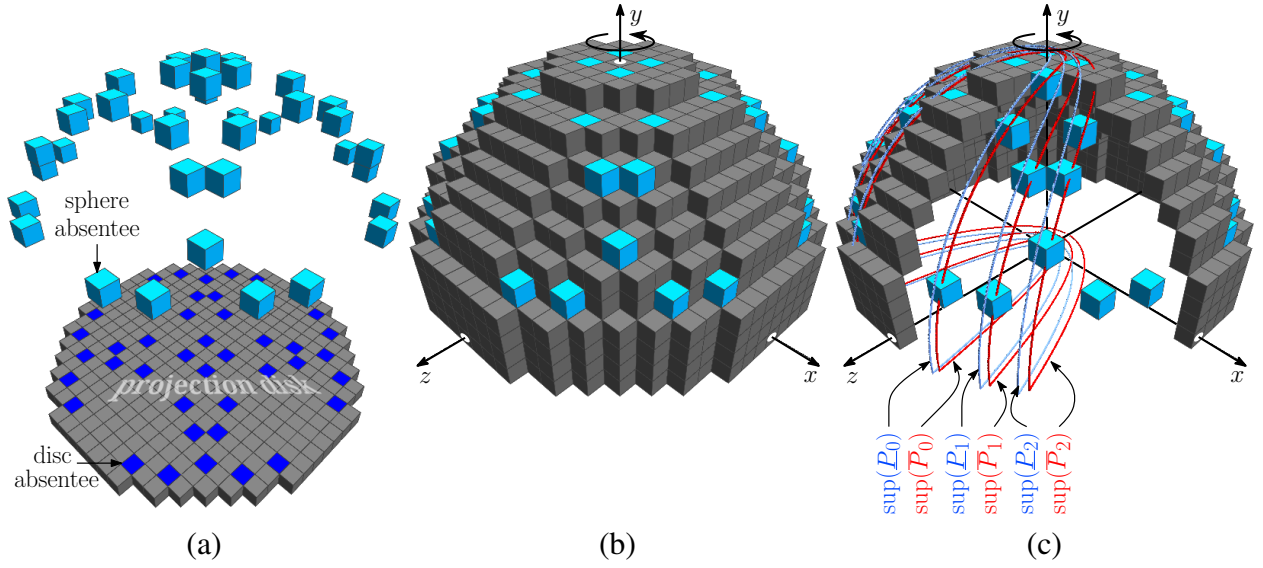


Figure 2: (a) One-to-one correspondence for  $r = 10$  between absentee-voxels (shown in red) in  $\mathcal{H}_U^Z(r)$  and absentee-pixels (shown in blue) in  $\mathcal{D}_U^Z(r)$ . (b) Hemisphere of  $r = 10$  after fixing absentees. (c) Parabolic surfaces of translation, produced by translating  $\text{sup}(P_{h,1})$  and  $\text{sup}(\bar{P}_{h,1})$ ,  $h = 0, 1, 2$ , along  $y$ -axis.

For Case 1, we get two concentric circles of radii differing by unity and lying on the same plane; the radii of the circles corresponding to  $p_i$  and  $p_{i+1}$  are  $x_i$  and  $(x_{i+1} = x_i + 1)$ . Hence, for Case 1, the absentee-voxels between two consecutive circles easily correspond to the absentee-pixels between  $\mathcal{C}^Z(o, x_i)$  and  $\mathcal{C}^Z(o, x_i + 1)$ .

For Case 2, the circle generated by  $p_{i+1}$  has radius  $x_{i+1} = x_i + 1$  and its plane lies one voxel apart w.r.t. the plane of the circle generated by  $p_i$ . Hence, if these two circles are projected on  $zx$ -plane, then the absentee-pixels lying between the projected circles have a correspondence with the absentee-voxels between the original circles.

For Case 3, we do not have an absentee, as the circles generated by  $p_i$  and  $p_{i+1}$  have the same radius ( $x_i = x_{i+1}$ ).

Hence, the count of absentee-voxels in  $\mathcal{H}_U^Z(r)$  is same as the count of absentee-pixels in  $\mathcal{D}_U^Z(r)$ . However, it may be noted that the count of voxels present in  $\mathcal{H}_U^Z(r)$  would be greater than the count of pixels present in  $\mathcal{D}_U^Z(r)$ , since for each circle of a particular radius  $r' \in \{0, 1, 2, \dots, r\}$  in  $\mathcal{D}_U^Z(r)$ , there would be one or more circles of radius  $r'$  (in succession) in  $\mathcal{H}_U^Z(r)$ . We have the lemma on the correspondence of absentee count in  $\mathcal{H}_U^Z(r)$  with that in  $\mathcal{D}_U^Z(r)$ .

**Lemma 1.** *If  $p(i, j, k)$  is an absentee-voxel in  $\mathcal{H}_U^Z(r)$ , then the pixel  $(i, k)$  obtained by projecting  $p$  on  $xz$ -plane is an absentee-pixel in  $\mathcal{D}_U^Z(r)$ .*

The above one-to-one correspondence between the absentees in the hemispherical surface for radius  $r = 10$  and the absentees related to the disc of radius  $r = 10$  is shown in Figure 2. This one-to-one correspondence between the absentee set in  $\mathcal{H}_U^Z(r)$  and that in  $\mathcal{D}_U^Z(r)$  leads to the following theorem.

**Theorem 3.** *The total count of absentee-voxels in  $\mathcal{H}_U^Z(r)$  is  $|\mathcal{A}^Z(r)| = \Theta(r^2)$ .*

*Proof.* Follows from Lemma 1 and Theorem 2.  $\square$

On taking the reflection of  $\mathcal{H}^{\mathbb{Z}}(r)$  about the  $zx$ -plane, we get the complementary hemisphere, namely  $\mathcal{H}'^{\mathbb{Z}}(r)$ . The set  $\mathcal{H}^{\mathbb{Z}}(r) \cup \mathcal{H}'^{\mathbb{Z}}(r)$  is the sphere,  $\mathcal{S}^{\mathbb{Z}}(r)$ , corresponding to which we get double the count of absentee-voxels compared to that in  $\mathcal{H}^{\mathbb{Z}}(r)$ . Hence, we have the following theorem.

**Theorem 4.** *The total count of absentee-voxels lying on  $\mathcal{S}_{\cup}^{\mathbb{Z}}(r)$  is given by*

$$|\mathcal{A}^{\mathbb{Z}^3}(r)| = 2|\mathcal{A}^{\mathbb{Z}^2}(r)| = 16 \sum_{k=0}^{m_r-1} |\mathcal{A}^{\mathbb{Z}^2}(r)| = \Theta(r^2).$$

*Proof.* Follows from Theorem 1 and Theorem 3.  $\square$

### 3.1. Characterizing the Absentee Family

We use the following lemmas from [4, 5] for deriving the necessary and sufficient conditions to decide whether a given voxel is an absentee or not.

**Lemma 2** (circle pixel [5]). *The squares of abscissae of the pixels with  $z = k$  in  $\mathcal{C}_1^{\mathbb{Z}}(r')$  drawn on  $zx$ -plane lie in the interval  $I_{r'-k}^{(r')} := [u_{r'-k}^{(r')}, v_{r'-k}^{(r')}]$ , where  $u_{r'-k}^{(r')} = r'^2 - k^2 - k$  and  $v_{r'-k}^{(r')} = r'^2 - k^2 + k$ .*

**Lemma 3** (absentee [4]). *A point  $(i, 0, k) \in \mathbb{Z}^3$  is an absentee on the  $zx$ -plane if and only if  $i^2$  lies in the integer interval  $J_{r'-k}^{(r')} := [v_{r'-k}^{(r')}, u_{r'+1-k}^{(r'+1)}]$  for some  $r' \in \mathbb{Z}^+$ .*

We have now the following theorem on the necessity and sufficiency for an absentee-voxel in  $\mathcal{S}_{\cup}^{\mathbb{Z}}(r)$ .

**Theorem 5.** *A voxel  $p(i, j, k)$  is an absentee if and only if  $i^2 \in J_{r'-k}^{(r')}$  for some  $r' \in \mathbb{Z}^+$  and  $r'^2 \in I_{r-j}^{(r)}$ .*

*Proof.* Lemma 1 implies that when  $p(i, j, k)$  is an absentee-voxel in  $\mathcal{H}_{\cup}^{\mathbb{Z}}(r)$ , then its projection pixel  $p'(i, k)$  on  $zx$ -plane is absentee-pixel in  $\mathcal{D}_{\cup}^{\mathbb{Z}}(r)$ . Hence, by Lemma 3,  $i^2$  lies in  $J_{r'-k}^{(r')}$  for some  $r' \in \mathbb{Z}^+$ . What now remains to check is the condition for  $y$ -coordinate of  $p$ . Observe that there exists a circle  $\mathcal{C}^{\mathbb{Z}}(c, r')$  centered at  $c = (0, j, 0)$  on the hemisphere such that the the projection of  $\mathcal{C}^{\mathbb{Z}}(c, r')$  on  $zx$ -plane is the circle of radius  $r'$  in  $\mathcal{D}_{\cup}^{\mathbb{Z}}(r)$ . Again  $p(i, j, k)$  and  $\mathcal{C}^{\mathbb{Z}}(c, r')$  lie on the same plane, i.e.,  $y = j$ . Hence, the pixel  $(r', j)$  must lie on the generating circular arc,  $\mathcal{C}_{1,2}^{\mathbb{Z}}(r)$ , and so by Lemma 2, we have  $r'^2 \in I_{r-j}^{(r)}$ .

Conversely, if  $i^2 \in J_{r'-k}^{(r')}$ , then  $p \notin \mathcal{H}_{\cup}^{\mathbb{Z}}(r)$ ; and if  $r'^2 \in I_{r-j}^{(r)}$  for some  $r' \in \{0, 1, 2, \dots, r\}$ , then  $p \in \mathcal{H}^{\mathbb{Z}}(r)$ , wherefore  $p$  is an absentee.  $\square$

An example of absentee-voxel is  $(2, 9, 4)$  in hemisphere of radius  $r = 10$  (Figure 2), since for  $k = 4$ , we have  $r' = 4$  for which  $v_{r'-k}^{(r')} = r'^2 - k^2 + k = 16 - 16 + 4 = 4$ ,  $u_{r'+1-k}^{(r'+1)} = (r' + 1)^2 - k^2 - k = 25 - 16 - 4 = 5$ , thus giving  $J_0^{(4)} = [4, 5) = [4, 4]$  in which lies the square

number  $4 = i^2$  and  $u_{r-j}^{(r)} = r^2 - j^2 - j = 10^2 - 9^2 - 9 = 10$ ,  $v_{r-j}^{(r)} = r^2 - j^2 + j = 10^2 - 9^2 + 9 = 28$ , thus giving  $I_{r-j}^{(r)} = [10, 28)$  which contains  $r'^2 = 16$ .

On the contrary,  $(3, 9, 4)$  is not an absentee-voxel, as for  $k = 4$ , there is no such  $r'$  for which  $J_{r'-4}^{(r')}$  contains  $3^2$ ; in fact, for  $k = 4$ , we get the interval  $I_{5-4}^{(5)} = [5^2 - 4^2 - 4, 5^2 - 4^2 + 4) = [5, 12]$  with  $r' = 5$ , which contains  $3^2$ , thereby making  $(3, 9, 4)$  a point on hemisphere of radius  $r = 10$  at the plane  $y = 9$ .

To characterize the absentees as a whole, we use Lemma 3 for the expanded form of (the lower and the upper limits of)  $J_{r'-k}^{(r')}$ . We replace  $r'$  by  $k + h$  and  $r' + 1$  by  $k + (h + 1)$ , where the  $h(\geq 0)$ th run of pixels in  $\mathcal{C}_1^{\mathbb{Z}}(r')$  drawn on  $zx$ -plane has  $z = k$  [5]. Thus,

$$\begin{aligned} v_{r'-k}^{(r')} &= (2h + 1)k + h^2, \\ u_{r'+1-k}^{(r'+1)} &= (2h + 1)k + (h + 1)^2. \end{aligned} \tag{1}$$

Hence, if  $p(i, 0, k)$  is a point in Octant 1 and lies on  $h^{\text{th}}$  run of  $\mathcal{C}_1^{\mathbb{Z}}(r')$ , then

$$i^2 < (2h + 1)k + h^2; \tag{2}$$

and if  $p(i, 0, k)$  is a point in Octant 1 and lies left of the  $(h + 1)^{\text{th}}$  run of  $\mathcal{C}_1^{\mathbb{Z}}(r' + 1)$ , then

$$i^2 < (2h + 1)k + (h + 1)^2. \tag{3}$$

Equations 2 and 3 correspond to two parabolic regions in the real ( $zx$ -)plane on replacing  $i$  and  $k$  by  $x$  and  $z$ , respectively,  $h$  being considered as a constant. These *open parabolic regions* are given by

$$\begin{aligned} \underline{P}_{h,1} : x^2 &< (2h + 1)z + h^2, \\ \overline{P}_{h,1} : x^2 &< (2h + 1)z + (h + 1)^2. \end{aligned} \tag{4}$$

The respective suprema of these two regions are given by two parabolas, namely  $\sup(\underline{P}_{h,1}) : x^2 = (2h + 1)z + h^2$  and  $\sup(\overline{P}_{h,1}) : x^2 = (2h + 1)z + (h + 1)^2$ . In 3D space, these two suprema correspond to two *parabolic surfaces of translation*, produced by translating  $\sup(\underline{P}_{h,1})$  and  $\sup(\overline{P}_{h,1})$  along  $y$ -axis, as shown in Figure 2c. Evidently, the absentees of  $\mathcal{H}_{\cup}^{\mathbb{Z}}(r)$  in Octant 1 and Octant 8 lie in the *half-open 3D parabolic region* given by  $P_h := \overline{P}_{h,1} \setminus \underline{P}_{h,1}$  for a given pair of  $k$  and  $h$ , i.e., for a given  $(r', k)$ -pair. The family of all the half-open 3D parabolic regions,  $P_0, P_1, P_2, \dots$ , thus contains all the absentees  $\mathcal{H}_{\cup}^{\mathbb{Z}}(r)$  in Octant 1 and Octant 8, as stated in the following theorem.

**Theorem 6.** *All the absentees of  $\mathcal{H}_{\cup}^{\mathbb{Z}}(r)$  in Octant 1 and Octant 8 lie in*

$$\mathcal{F} := \{P_h \cap \mathbb{Z}_1^3 : h = 0, 1, 2, \dots\}.$$

*Proof.* Follows from Theorem 5 and Eqn. 4. □



---

**Algorithm 1:** (AVH) Fixing absentee-voxels in the hemisphere

---

**Input:** Generating circular arc,  $\mathcal{C}_{1,2}^{\mathbb{Z}}(r) := \{p_1, p_2, \dots, p_{n_r}\}$

**Output:** Absentee-voxels in  $\mathcal{H}_{\cup}^{\mathbb{Z}}(r)$

```
1  $\mathcal{A}^{\mathbb{Z}^3}(r) \leftarrow \emptyset$ 
2 for  $t = 1, 2, \dots, n_r - 1$  do
3   if  $i_{t+1} > i_t$  then
4      $\mathcal{A}^{\mathbb{Z}^3}(r) \leftarrow \mathcal{A}^{\mathbb{Z}^3}(r) \cup \text{ACC}(\mathcal{C}_{1,2}^{\mathbb{Z}}(r), t)$ 
5 return  $\mathcal{A}^{\mathbb{Z}^3}(r)$ 
```

---

---

**Procedure**  $\text{ACC}(\mathcal{C}_{1,2}^{\mathbb{Z}}(r), t)$ 

---

```
1  $A \leftarrow \emptyset, r \leftarrow i_t$ 
2 int  $i \leftarrow 0, k \leftarrow r, s \leftarrow 0, w \leftarrow r - 1$ 
3 int  $l \leftarrow 2w$ 
4 while  $k \geq i$  do
5   repeat
6      $s \leftarrow s + 2i + 1$ 
7      $i \leftarrow i + 1$ 
8   until  $s \leq w$ ;
9   if  $i^2 \in J_{r-k}^{(r)}$  and  $k \geq i$  then
10     $A \leftarrow A \cup \{(i', j_t, k') : \{|i'|\} \cup \{|k'|\} = \{i, k\}\}$ 
11     $w \leftarrow w + l, l \leftarrow l - 2, k \leftarrow k - 1$ 
12 return  $A$ 
```

---

### 3.2. Fixing the Absentee-Voxels

Algorithm 1 (AVH) shows the steps for fixing the absentee-voxels corresponding to the hemisphere  $\mathcal{H}_{\cup}^{\mathbb{Z}}(r)$  having radius  $r$ . The generating curve, which is an input to this algorithm, is the circular arc,  $\mathcal{C}_{1,2}^{\mathbb{Z}}(r)$ . This circular arc is a (ordered) sequence of points,  $\{p_t(i_t, j_t, 0) \in \mathbb{Z}^3 : t = 1, 2, \dots, n_r\}$ , whose first point is  $p_1(0, r, 0)$  and last point is  $p_{n_r}(r, 0, 0)$ . The point  $p_{t+1}$  can have  $i_{t+1}$  either same as  $i_t$  of the previous point  $p_t$  or greater than  $i_t$  by unity. For the former case, there is no absentee between the two circles generated by  $p_t$  and  $p_{t+1}$ . For the latter, the absentees are computed by invoking the procedure ACC, as shown in Step 4 of Algorithm 1.

The procedure ACC finds the absentee-voxels between two concentric circles,  $\mathcal{C}_{y=j}^{\mathbb{Z}}(c, i)$  and  $\mathcal{C}_{y=j}^{\mathbb{Z}}(c, i + 1)$  of radii  $i$  and  $i + 1$ , each centered at  $(0, j, 0)$  on  $y = j$  plane. The set of all absentees between these two circles is denoted by  $A$ . As an absentee lies just after the end of a *voxel-run* corresponding to the interval  $I_{r-j}^{(r)}$  (Lemma 2), the procedure ACC first computes the voxel-run in the plane  $y = j$  (Steps 5–8). Then, in Step 9, it determines whether the next voxel is an absentee in Octant 1, using Lemma 3. For each absentee-voxel in Octant 1, the absentees in all other octants are included in  $A$ , as shown in Step 10. Figure 2(a) shows the hemisphere for  $r = 10$ , whose absentees (shown in red) have been fixed by Algorithm 1.

#### 4. Absentees in a Solid Sphere

As mentioned earlier in Sec. 2, the absentee-voxels in a solid sphere  $\mathbf{S}_{\cup}^{\mathbb{Z}}(r)$  can also be characterized using the set of disc absentees,  $\mathcal{A}^{\mathbb{Z}^2}(r)$ . The set of voxels defining  $\mathbf{S}_{\cup}^{\mathbb{Z}}(r)$  is given by the union of the voxel sets corresponding to the complete spheres of radii  $0, 1, 2, \dots, r$  (Definition 7).

To find the absentees in  $\mathbf{S}_{\cup}^{\mathbb{Z}}(r)$ , we consider its lower (or upper) hemisphere,  $\mathbf{H}_{\cup}^{\mathbb{Z}}(r)$ . Three-fourth of the upper hemisphere and the entire lower hemisphere of  $\mathbf{S}_{\cup}^{\mathbb{Z}}(r)$  are shown in Figure 3a. Observe that the set of voxels of  $\mathbf{H}_{\cup}^{\mathbb{Z}}(r)$  lying in the 1st quadrant of  $xy$ -,  $yz$ -, or  $zx$ -plane is given by the union of voxels comprising those arcs of the complete spheres which lie in the 1st quadrant of the concerned plane. Hence, the above set of voxels is same as the subset of  $\mathcal{D}_{\cup}^{\mathbb{Z}}(r)$  lying in this quadrant, or, the absentee-voxels in this quadrant are in one-to-one correspondence with the disc absentees in  $\mathcal{D}_{\cup}^{\mathbb{Z}}(r)$  (Figure 2a). The absentees in this quadrant are, however, characterized depending on the coordinate plane, as follows.

- (AL) For each absentee  $p(i, 0, k)$  in the 1st quadrant of  $zx$ -plane, there are absentees in  $\mathbf{H}_{\cup}^{\mathbb{Z}}(r)$ , which comprise an *absentee line*, given by  $\mathbf{L}_{(i,k)}^{\mathbb{Z}^3} = \{(i, j, k) : j' < j \leq 0 \wedge (i, j', k) \in \mathbf{H}_{\cup}^{\mathbb{Z}}(r)\}$ . These absentee lines are shown in yellow in the lower hemisphere in Figure 3b.
- (AC) For each absentee  $p(i, j, 0)$  in the 1st quadrant of  $xy$ -plane, there are absentees in  $\mathbf{H}_{\cup}^{\mathbb{Z}}(r)$ , which comprise an *absentee circle*, given by  $\mathbf{C}_{(i,j)}^{\mathbb{Z}^3} = \{(i', j, k') : (i', j, k') \in \mathcal{C}_{y=j}^{\mathbb{Z}}(c, i) \wedge c = (0, j, 0)\}$ . These absentee circles, shown in red in the upper hemisphere in Figure 3b, pass through the absentees in the 1st quadrant of  $yz$ -plane.

##### 4.1. Characterizing the Absentee Family

We characterize here the family of absentee-voxels comprising the absentee lines that comprising the absentee circles. For this, we need the following theorems on the necessity and sufficiency for an absentee belonging to an absentee line or an absentee circle in  $\mathbf{H}_{\cup}^{\mathbb{Z}}(r)$ .

**Theorem 7.** A voxel  $p(i, j, k)$  belongs to an absentee line if and only if  $i^2 \in J_{r'-k}^{(r')}$  for some  $r' \in \mathbb{Z}^+$  and  $0 \leq j \leq \lfloor \sqrt{r'} \rfloor + 1$ .

*Proof.* From (AL), if  $p(i, j, k)$  belongs to an absentee line  $\mathbf{L}_{(i,k)}^{\mathbb{Z}^3}$ , then  $p(i, 0, k)$  is a disc absentee on  $zx$ -plane. Hence, by Lemma 3,  $i^2 \in J_{r'-k}^{(r')}$  for some  $r' \in \mathbb{Z}^+$ . Further,  $\mathbf{L}_{(i,k)}^{\mathbb{Z}^3}$  lies between two complete hemispheres, namely  $\mathbf{H}_{\cup}^{\mathbb{Z}}(r')$  and  $\mathbf{H}_{\cup}^{\mathbb{Z}}(r' + 1)$ , where  $r' = \lfloor i^2 + k^2 - k \rfloor$ . In particular,  $\mathbf{L}_{(i,k)}^{\mathbb{Z}^3}$  lies between the surface of revolution generated by the topmost run of (generatrix)  $\mathcal{C}_{34}^{\mathbb{Z}}(r' + 1)$  and that generated by the topmost run of  $\mathcal{C}_{34}^{\mathbb{Z}}(r')$ . Hence, the value of  $j$  can be at most the length of the topmost run of  $\mathcal{C}_{34}^{\mathbb{Z}}(r' + 1)$ , which is  $\lfloor \sqrt{r'} \rfloor + 1$  by Lemma 2.

Conversely, if  $i^2 \in J_{r'-k}^{(r')}$  for some  $r' \in \mathbb{Z}^+$ , then by Lemma 3,  $p(i, 0, k)$  is a disc absentee on  $zx$ -plane. Hence, if  $0 \leq j \leq \lfloor \sqrt{r'} \rfloor + 1$ , then from (AL),  $(i, j, k)$  belongs to  $\mathbf{L}_{(i,k)}^{\mathbb{Z}^3}$  that lies between the surfaces of revolution generated by  $\mathcal{C}_{34}^{\mathbb{Z}}(r' + 1)$  and  $\mathcal{C}_{34}^{\mathbb{Z}}(r')$ .  $\square$

**Theorem 8.** A voxel  $p(i, j, k)$  belongs to an absentee circle if and only if  $i^2 \in I_{r'-k}^{(r')}$  for some  $r' \in \mathbb{Z}^+$  such that  $r'^2 \in J_{r''-j}^{(r'')}$  for some  $r'' \in \mathbb{Z}^+$ .

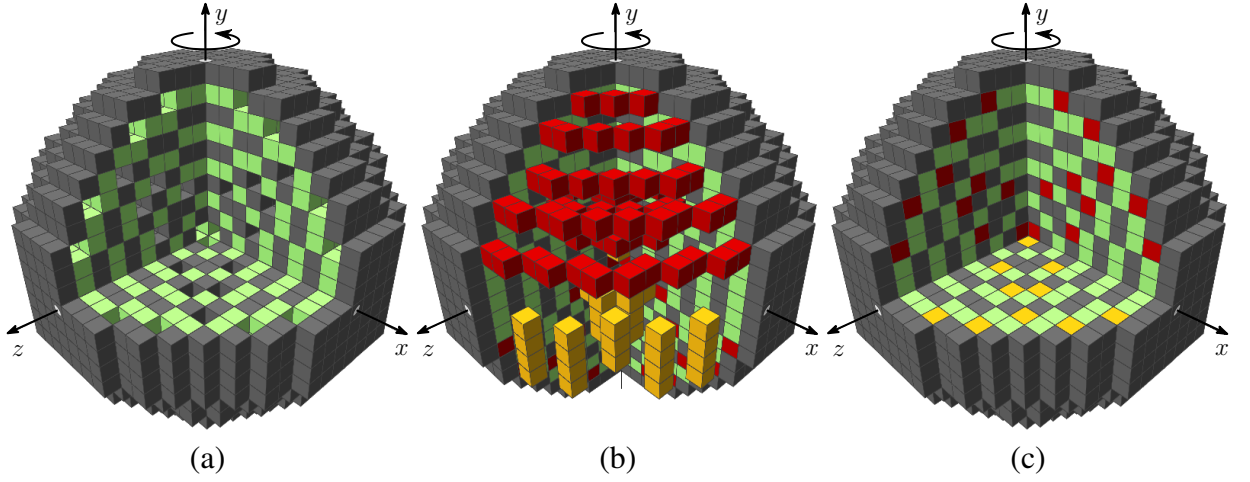


Figure 3: Covering a solid sphere ( $r = 10$ ) by concentric complete spheres. (a) Concentric complete spheres for  $r = 0, 1, \dots, 10$ . (b) Absentee lines (yellow) in the lower hemisphere and absentee circles (red) in the upper hemisphere. (c) Complete solid sphere after fixing the absentee lines and absentee circles.

*Proof.* From (AC), if  $p(i, j, k)$  belongs to an absentee circle, then that absentee circle  $\mathcal{C}^{\mathbb{Z}}(r')$  lies on the plane  $y = j$ , where  $(r', j)$  is a disc absentee in  $\mathcal{D}_{\mathbb{U}}^{\mathbb{Z}}(r)$  in  $xy$ -plane. Hence, by Lemma 3,  $r'^2 \in J_{r''-j}^{(r'')}$  for some  $r'' \in \mathbb{Z}^+$ . Further, since  $p \in \mathcal{C}^{\mathbb{Z}}(r')$ , we get  $i^2 \in I_{r'-k}^{(r')}$  by Lemma 2.

Conversely, if  $r'^2 \in J_{r''-j}^{(r'')}$  for some  $r'' \in \mathbb{Z}^+$ , then by Lemma 3,  $(r', j)$  is a disc absentee on  $xy$ -plane, and so  $\mathcal{C}^{\mathbb{Z}}(r')$  is an absentee circle. Hence, by Lemma 2, if  $i^2 \in I_{r'-k}^{(r')}$ , then  $p \in \mathcal{C}^{\mathbb{Z}}(r')$ , or,  $p$  belongs to an absentee circle.  $\square$

The absentee circles are characterized based on locations of their corresponding disc absentees on (real)  $xy$ -plane. The digital disc has eight octants. All the absentee circles corresponding to the disc absentees in Octant 1 include the disc absentees in Octant 8. Reflection of these absentee circles simply gives all the absentee circles corresponding to the disc absentees in Octant 4 (and 5), and hence the characterization of absentee circles corresponding to Octant 4 is very much similar to that corresponding to Octant 1. But the characterization of absentee circles corresponding to Octant 2 (and 7) is different and it can be used to obtain the characterization corresponding to Octant 3 (and 6) also. Hence, following are two theorems on characterization of absentee circles—one for Octant 1 and another for Octant 2.

**Theorem 9.** *All the absentee circles of  $\mathcal{S}_{\mathbb{U}}^{\mathbb{Z}}(r)$  corresponding to Octant 1 lie in*

$$\mathcal{F}_1 := \{\mathbf{P}_{h,1} \cap \mathbb{Z}_1^3 : h = 0, 1, 2, \dots\} \quad (5)$$

where,

$$\mathbf{P}_{h,1} = \overline{\mathbf{P}}_{h,1} \setminus \underline{\mathbf{P}}_{h,1} \quad (6)$$

such that

$$\begin{aligned} \underline{\mathbf{P}}_{h,1} : x^2 + z^2 &< (2h+1)y + h^2, \\ \overline{\mathbf{P}}_{h,1} : x^2 + z^2 &< (2h+1)y + (h+1)^2. \end{aligned} \quad (7)$$

*Proof.* We use Theorem 8 for the expanded forms of the lower and the upper limits of  $J_{r''-j}^{(r'')}$ . Using Lemma 3 and replacing  $r'' - j$  by  $h$ , we get

$$\begin{aligned} v_{r''-j}^{(r'')} &= (2h+1)j + h^2, \\ u_{r''+1-j}^{(r''+1)} &= (2h+1)j + (h+1)^2. \end{aligned} \quad (8)$$

Hence, if  $p(i, j = r'' - h, 0)$  is a point on or inside  $\mathcal{C}_1^{\mathbb{Z}}(r'')$  but strictly inside  $\mathcal{C}_1^{\mathbb{Z}}(r'' + 1)$ , then

$$\begin{aligned} i^2 &< (2h+1)j + h^2, \\ i^2 &< (2h+1)j + (h+1)^2. \end{aligned} \quad (9)$$

Equation 9 corresponds to two *open parabolic regions* on the  $xy$ -plane, on replacing  $i$  and  $j$  by  $x$  and  $y$  respectively,  $h$  being considered as a constant. These open parabolic regions are given by

$$\begin{aligned} \underline{P}_{h,1} : x^2 &< (2h+1)y + h^2, \\ \overline{P}_{h,1} : x^2 &< (2h+1)y + (h+1)^2. \end{aligned} \quad (10)$$

The respective suprema of these two regions are given by two parabolas, namely  $\sup(\underline{P}_{h,1}) : x^2 = (2h+1)y + h^2$  and  $\sup(\overline{P}_{h,1}) : x^2 = (2h+1)y + (h+1)^2$ . On rotating  $\sup(\underline{P}_{h,1})$  and  $\sup(\overline{P}_{h,1})$  about  $y$ -axis, we get two paraboloidal surfaces that enclose two *open paraboloidal spaces* given by Eqn. 7. Evidently, the absentee circles corresponding to the disc absentees in Octant 1 and Octant 8 lie in the *half-open paraboloidal space*  $\mathbf{P}_{h,1}$ , given by Eqn. 6, for a given value of  $h (= r'' - j)$ . Hence, the family  $\mathcal{F}_1$  of all these half-open paraboloidal spaces is given by Eqn. 5, which contains all the aforesaid absentee circles. An illustration is shown in Figure 4 for  $r = 10$ .  $\square$

**Theorem 10.** *All the absentee circles of  $\mathbf{S}_{\mathbb{U}}^{\mathbb{Z}}(r)$  corresponding to Octant 2 lie in*

$$\mathcal{F}_2 := \{\mathbf{P}_{h,2} \cap \mathbb{Z}_1^3 : h = 0, 1, 2, \dots\} \quad (11)$$

where,

$$\mathbf{P}_{h,2} = \overline{\mathbf{P}}_{h,2} \setminus \underline{\mathbf{P}}_{h,2} \quad (12)$$

such that

$$\begin{aligned} \underline{\mathbf{P}}_{h,2} : y^2 &< (2h+1)\sqrt{x^2 + z^2} + h^2, \\ \overline{\mathbf{P}}_{h,2} : y^2 &< (2h+1)\sqrt{x^2 + z^2} + (h+1)^2. \end{aligned} \quad (13)$$

*Proof.* In Octant 1, the parabolic regions containing the disc absentees have all their axes coinciding with  $y$ -axis. On the contrary, in Octant 2, the axes of the parabolic regions containing the disc absentees all coincide with  $x$ -axis. Hence, for each absentee  $(i, j)$  in Octant 2,  $j^2 \in J_{r''-i}^{(r'')}$ . We use Theorem 8 as before, and using Lemma 3 and replacing  $r'' - i$  by  $h$ , we get

$$\begin{aligned} v_{r''-i}^{(r'')} &= (2h+1)i + h^2, \\ u_{r''+1-i}^{(r''+1)} &= (2h+1)i + (h+1)^2. \end{aligned} \quad (14)$$

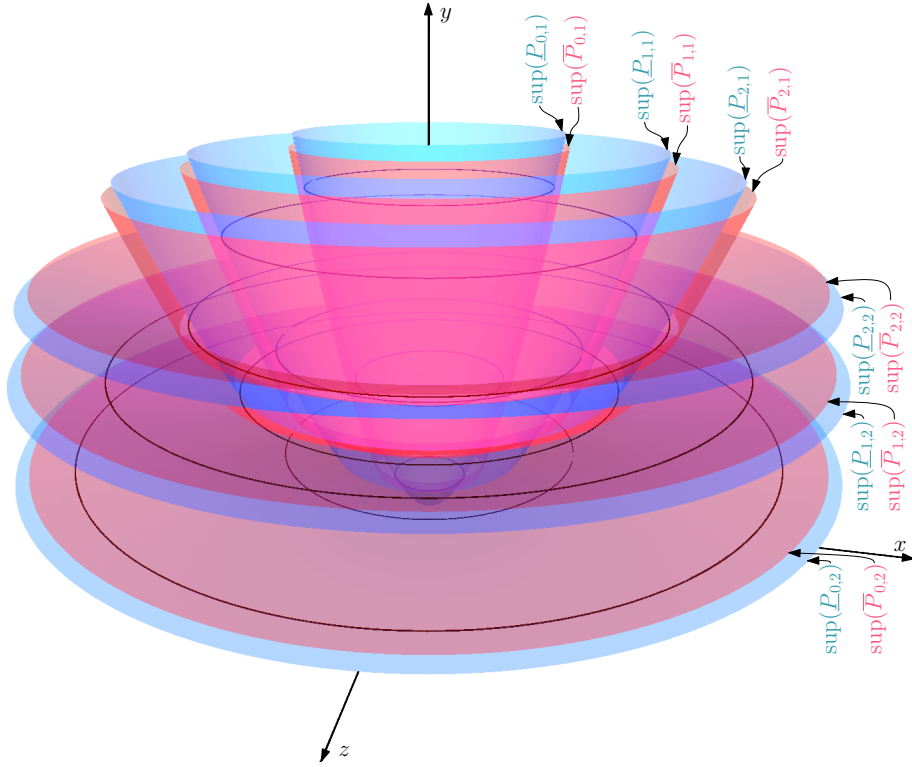


Figure 4: Illustration of Theorem 9 and Theorem 10 for  $r = 10$ . The paraboloidal surfaces  $\text{sup}(\underline{P}_{h,1})$  and  $\text{sup}(\underline{P}_{h,2})$  are shown in blue, and  $\text{sup}(\overline{P}_{h,1})$  and  $\text{sup}(\overline{P}_{h,2})$  in red;  $h = 0, 1, 2$  as  $r = 10$ . For clarity, the absentee circles lying in the open paraboloidal spaces are shown as real circles.

Hence, if  $p(i = r'' - h, j, 0)$  is a point on or inside  $\mathcal{C}_1^{\mathbb{Z}}(r'')$  but strictly inside  $\mathcal{C}_1^{\mathbb{Z}}(r'' + 1)$ , then

$$\begin{aligned} j^2 &< (2h + 1)i + h^2, \\ j^2 &< (2h + 1)i + (h + 1)^2. \end{aligned} \tag{15}$$

As explained in Theorem 9, Eqn. 15 corresponds to two *open parabolic regions* given by

$$\begin{aligned} \underline{P}_{h,2} : y^2 &< (2h + 1)x + h^2, \\ \overline{P}_{h,2} : y^2 &< (2h + 1)x + (h + 1)^2. \end{aligned} \tag{16}$$

The respective suprema of these two regions are two parabolas, namely  $\text{sup}(\underline{P}_{h,2}) : y^2 = (2h + 1)x + h^2$  and  $\text{sup}(\overline{P}_{h,2}) : y^2 = (2h + 1)x + (h + 1)^2$ . On rotating  $\text{sup}(\underline{P}_{h,2})$  and  $\text{sup}(\overline{P}_{h,2})$  again about  $y$ -axis, we get two paraboloidal surfaces that enclose two *open paraboloidal spaces* given by Eqn. 7. The absentee circles corresponding to the disc absentees in Octant 2 lie in the *half-open paraboloidal space*  $\mathbf{P}_{h,2}$ , given by Eqn. 12, for a given value of  $h(= r'' - i)$ . As in Theorem 9, the family  $\mathcal{F}_2$ , given by Eqn. 11, contains all the absentee circles corresponding to Octant 2. See Figure 4 for an illustration with  $r = 10$ .  $\square$

#### 4.2. Absentee Count

We first have the following lemma on the count of absentee lines and that of absentee circles.

**Lemma 4.** *The respective counts of absentee lines and absentee circles in  $\mathbf{H}_{\mathbb{U}}^{\mathbb{Z}}(r)$  are  $|\mathcal{A}^{\mathbb{Z}^2}(r)|$  and  $\frac{1}{4}|\mathcal{A}^{\mathbb{Z}^2}(r)|$ .*

Using Lemma 4, we derive the count of absentee-voxels in  $\mathbf{S}_{\mathbb{U}}^{\mathbb{Z}}(r)$ , as stated in the following theorem.

**Theorem 11.** *The count of all absentee-voxels in  $\mathbf{S}_{\mathbb{U}}^{\mathbb{Z}}(r)$  is  $\Theta(r^3)$ .*

*Proof.* We first count the absentee-voxels comprising the absentee lines in  $\mathbf{H}_{\mathbb{U}}^{\mathbb{Z}}(r)$ . From Theorem 7, the count of voxels in  $\mathbf{L}_{(i,k)}^{\mathbb{Z}^3}$  is given by the length of the topmost run of  $\mathcal{C}_{34}^{\mathbb{Z}}(r' + 1)$ , which is  $\lfloor \sqrt{r'} \rfloor + 1$  by Lemma 2.

From Theorem 2, the count of disc absentees in  $\mathcal{D}_{\mathbb{U}}^{\mathbb{Z}}(r')$  is  $\Theta(r'^2)$ , which implies that the count of disc absentees between  $\mathcal{C}^{\mathbb{Z}}(r')$  and  $\mathcal{C}^{\mathbb{Z}}(r' + 1)$  is  $\Theta(r')$ . Hence, the count of absentee-voxels comprising all the absentee lines in  $\mathbf{H}_{\mathbb{U}}^{\mathbb{Z}}(r)$  is

$$\sum_{r'=1}^r \Theta(r')\Theta(\sqrt{r'}) = \sum_{r'=1}^r \Theta(r'^{3/2}) = \Theta\left(\sum_{r'=1}^r r'^{3/2}\right) = \Theta(r^{5/2}), \quad (17)$$

since  $\sum_{r'=1}^r r'^{3/2} > \sum_{r'=\lfloor r/2 \rfloor}^r r'^{3/2}$ , or,  $\sum_{r'=1}^r r'^{3/2} = \Omega(r^{5/2})$ ,

and  $\sum_{r'=1}^r r'^{3/2} < \sum_{r'=1}^r (r)^{3/2}$ , or,  $\sum_{r'=1}^r r'^{3/2} = O(r^{5/2})$ .

Now we count the absentee-voxels comprising the absentee circles in  $\mathbf{H}_{\mathbb{U}}^{\mathbb{Z}}(r)$ . From (AC), each absentee  $p(i, j, 0)$  corresponds to an absentee circle  $\mathbf{C}_{(i,j)}^{\mathbb{Z}^3}$ , which has radius  $i$  and lies on the plane  $y = j$ . Its symmetric absentee  $p'(j, i, 0)$  corresponds to another absentee circle  $\mathbf{C}_{(j,i)}^{\mathbb{Z}^3}$ , which has radius  $j$  and lies on the plane  $y = i$ . Voxel count of these two absentee circles is  $\Theta(i) + \Theta(j) = \Theta(i + j)$ , which is asymptotically same as the voxel count of  $\mathbf{C}_{(r',r',0)}^{\mathbb{Z}^3}$ , where  $r' = i + j$ . As explained above, the count of disc absentees between  $\mathcal{C}^{\mathbb{Z}}(r')$  and  $\mathcal{C}^{\mathbb{Z}}(r' + 1)$  is  $\Theta(r')$ , and for each of these disc absentees,  $i + j = \Theta(r')$ . Hence, the count of absentee-voxels comprising all the absentee circles in  $\mathbf{H}_{\mathbb{U}}^{\mathbb{Z}}(r)$  is

$$\sum_{r'=1}^r \Theta(r')\Theta(r') = \sum_{r'=1}^r \Theta((r')^2) = \Theta(r^3). \quad (18)$$

On doubling the absentee count as obtained above for  $\mathbf{H}_{\mathbb{U}}^{\mathbb{Z}}(r)$ , we get the count of all absentees in  $\mathbf{S}_{\mathbb{U}}^{\mathbb{Z}}(r)$  as  $\Theta(r^3)$ .  $\square$

#### 4.3. Fixing the Absentee Lines and Circles

Algorithm 2 (AVS) shows the steps for fixing the absentee lines and absentee circles corresponding to the solid sphere  $\mathbf{S}_{\mathbb{U}}^{\mathbb{Z}}(r)$  having radius  $r$ . For each disc absentee in Octant 1 on  $zx$ -plane, there are four or eight absentee lines, which are computed by invoking the procedure AbLine, as

---

**Algorithm 2:** (AVS) Fixing absentee-voxels in solid sphere

---

**Input:** Radius  $r$  of a solid sphere

**Output:** Set of the absentees

```
1  $\mathbf{A}^{\mathbb{Z}^3}(r) \leftarrow \emptyset$ 
2 int  $i \leftarrow 0, j \leftarrow r, s \leftarrow 0, w \leftarrow r - 1, h \leftarrow 0, i_a, j_a$ 
3 int  $l \leftarrow 2w$ 
4 while  $j \geq i$  do
5   repeat
6      $s \leftarrow s + 2i + 1, i \leftarrow i + 1$ 
7   until  $s \leq w$ ;
8    $i_a \leftarrow i - 1, j_a \leftarrow j$ 
9   while  $j_a \geq i_a$  do
10    if  $i_a^2 < (2h + 1)j_a + h^2$  then
11       $j_a \leftarrow j_a - 1$ 
12    else
13      if  $i_a^2 < (2h + 1)j_a + (h + 1)^2$  then
14         $\mathbf{A}^{\mathbb{Z}^3}(r) \leftarrow \mathbf{A}^{\mathbb{Z}^3}(r) \cup \text{AbLine}(i_a, j_a, j_a + h)$ 
15        if  $i_a = j_a$  then
16           $\mathbf{A}^{\mathbb{Z}^3}(r) \leftarrow \mathbf{A}^{\mathbb{Z}^3}(r) \cup \text{AbCircle}(i_a, j_a)$ 
17        else
18           $\mathbf{A}^{\mathbb{Z}^3}(r) \leftarrow \mathbf{A}^{\mathbb{Z}^3}(r) \cup \text{AbCircle}(i_a, j_a)$ 
19           $\mathbf{A}^{\mathbb{Z}^3}(r) \leftarrow \mathbf{A}^{\mathbb{Z}^3}(r) \cup \text{AbCircle}(j_a, i_a)$ 
20         $i_a \leftarrow i_a - 1$ 
21     $w \leftarrow w + l, l \leftarrow l - 2, j \leftarrow j - 1, h \leftarrow h + 1$ 
22 return  $\mathbf{A}^{\mathbb{Z}^3}(r)$ 
```

---

shown in Step 14 of Algorithm 2. Again, for each disc absentee in Octant 1 and Octant 2 on  $xy$ -plane, there are two absentee circles—one for the upper hemisphere and another for the lower. These absentee circles are computed by invoking the procedure `AbCircle`, as shown in Step 15 of Algorithm 2.

The procedure `AbLine` takes the coordinates  $(i_a, k_a)$  of a disc absentee as input. It also takes a radius  $r$  as the third argument, such that  $(i_a, k_a)$  lies between  $\mathcal{C}^{\mathbb{Z}}(r)$  and  $\mathcal{C}^{\mathbb{Z}}(r + 1)$ . Based on these, it computes the voxels comprising the absentee lines  $\left\{ \mathbf{L}_{(i'_a, k'_a)}^{\mathbb{Z}^3} : \{|i'_a|\} \cup \{|k'_a|\} = \{i_a, k_a\} \right\}$ .

The procedure `AbCircle` requires only the coordinates  $(i_a, j_a)$  of a disc absentee as input. If the disc absentee has  $i_a = j_a$ , then there arises one absentee circle with radius  $i_a$  and center  $(0, j_a, 0)$ ; otherwise, there are two absentee circles with radius  $i_a$  and  $j_a$ , and centered at  $(0, j_a, 0)$  and  $(0, i_a, 0)$ , respectively.

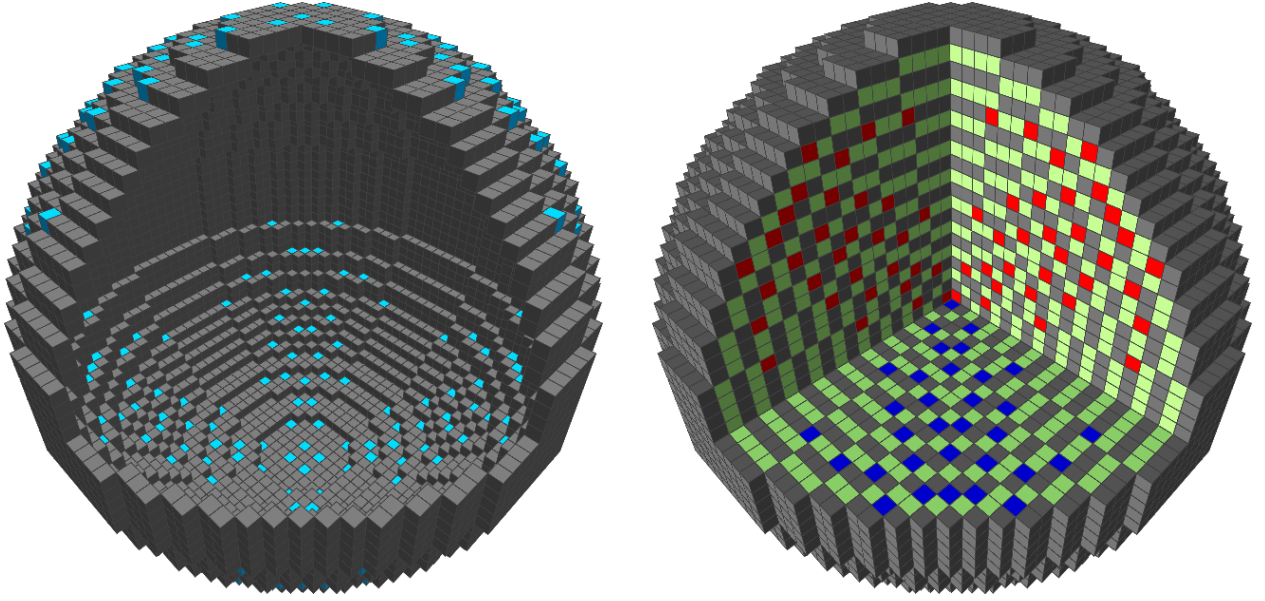


Figure 5: Sphere and solid sphere of radius 20 generated by the proposed algorithm.

---

**Procedure** AbLine( $i_a, k_a, r$ )

---

```

1  $A \leftarrow \emptyset$ 
2 int  $j_a \leftarrow 0$ 
3 while  $j_a \leq \lfloor \sqrt{r} \rfloor + 1$  do
4    $A \leftarrow A \cup \{(i'_a, j'_a, k'_a) : \{|i'_a|\} \cup \{|k'_a|\} = \{i_a, k_a\} \wedge j_a = |j'_a|\}$ 
5    $j_a \leftarrow j_a + 1$ 
6 return  $A$ 

```

---



---

**Procedure** AbCircle( $i_a, j_a$ )

---

```

1  $A \leftarrow \emptyset, r \leftarrow i_a$ 
2 int  $i_a \leftarrow 0, k_a \leftarrow r, s \leftarrow 0, w \leftarrow r - 1$ 
3 int  $l \leftarrow 2w$ 
4 while  $k_a \geq i_a$  do
5   repeat
6      $A \leftarrow A \cup \{(i'_a, j_a, k'_a) : \{|i'_a|\} \cup \{|k'_a|\} = \{i_a, k_a\} \wedge j_a = |j'_a|\}$ 
7      $s \leftarrow s + 2i_a + 1, i_a \leftarrow i_a + 1$ 
8   until  $s \leq w$ ;
9    $w \leftarrow w + l, l \leftarrow l - 2, k_a \leftarrow k_a - 1$ 
10 return  $A$ 

```

---

## 5. Test Results and Conclusion

We have implemented Algorithm 1 and Algorithm 2 to generate absentee-free spheres and solid spheres. Figure 5 shows (absentee-free) instances of a sphere and a solid sphere generated by Algorithm 1 for radius 20.



Table 1: Exact counts of voxels in  $\mathcal{S}_{\cup}^{\mathbb{Z}}(r)$ ,  $\mathcal{A}^{\mathbb{Z}^3}(r)$ , and  $\mathcal{S}^{\mathbb{Z}}(r)$ .

$r$	$ \mathcal{S}_{\cup}^{\mathbb{Z}}(r) $	$2 \mathcal{A}^{\mathbb{Z}^3}(r) $	$ \mathcal{S}^{\mathbb{Z}}(r) $	$r$	$ \mathcal{S}_{\cup}^{\mathbb{Z}}(r) $	$2 \mathcal{A}^{\mathbb{Z}^3}(r) $	$ \mathcal{S}^{\mathbb{Z}}(r) $
0	1	0	1	1200	14543190	902056	15445246
1	6	0	6	1300	17063386	1058408	18121794
2	46	8	54	1400	19796562	1227664	21024226
3	82	8	90	1500	22720358	1409144	24129502
4	170	8	178	1600	25858590	1603424	27462014
5	254	24	278	1700	29186106	1810216	30996322
6	330	24	354	1800	32729258	2029288	34758546
7	498	40	538	1900	36460174	2261192	38721366
8	614	40	654	2000	40391978	2505328	42897306
9	830	48	878	2100	44542482	2762328	47304810
10	1002	80	1082	2200	48877878	3031440	51909318
20	3978	256	4234	2300	53433334	3313344	56746678
30	8962	560	9522	2400	58172210	3607600	61779810
40	16310	1016	17326	2500	63132842	3914608	67047450
50	25374	1592	26966	2600	68275238	4234008	72509246
60	36438	2296	38734	3000	90906366	5637120	96543486
70	49510	3080	52590	3500	123729002	7672616	131401618
80	64526	3992	68518	4000	161600518	10021480	171621998
90	81582	5080	86662	4500	204521258	12683288	217204546
100	100622	6248	106870	5000	252490950	15658504	268149454
200	404262	25104	429366	5500	305509450	18946648	324456098
300	908250	56320	964570	6000	363576838	22548008	386124846
400	1617026	100304	1717330	6500	426693594	26462560	453156154
500	2524486	156608	2681094	7000	494859006	30690136	525549142
600	3638230	225456	3863686	7500	568134414	35231256	603365670
700	4949282	307064	5256346	8000	646401914	40085200	686487114
800	6461350	400768	6862118	8500	729718814	45252704	774971518
900	8182310	507392	8689702	9000	818084450	50732656	868817106
1000	10097978	626304	10724282	9500	911499582	56526944	968026526
1100	12223938	757888	12981826	10000	1009962778	62620784	1072583562

We have performed experiments to compute the exact counts of absentee-voxels and sphere voxels for increasing radius of spheres of revolution. Table 1 shows the counts of voxels in  $\mathcal{S}_{\cup}^{\mathbb{Z}}(r)$ ,  $\mathcal{A}^{\mathbb{Z}^3}(r)$ , and  $\mathcal{S}^{\mathbb{Z}}(r)$ , for  $r$  up to 10000. We have also plotted these counts against radius  $r$  in Figure 6. These experimental results reinforce our analytical findings that all the three counts have a quadratic dependency on  $r$ . The relative counts of absentee-voxels corresponding to digital spheres of revolution for radius up to 10000 are tabulated in Table 2 and plotted in Figure 7. In Table 2, the relative count  $\mathcal{A}^{\mathbb{Z}^3}(r)/\mathcal{S}^{\mathbb{Z}}(r)$  is denoted by  $\alpha_r$ . We observe from these data that with the increasing radius, the value of relative count for solid sphere tends to 0.058 approximately.

We have also generated through our experiments the exact counts of absentee-voxels and sphere voxels corresponding to solid spheres of revolution. The counts of voxels in  $\mathbf{S}_{\cup}^{\mathbb{Z}}(r)$ ,  $\mathbf{A}^{\mathbb{Z}^3}(r)$ , and  $\mathbf{S}^{\mathbb{Z}}(r)$ , for  $r$  up to 800, are shown in Table 3 and plotted in Figure 8. Similar to the previous set of results, these experimental results also reinforce our analytical findings that all the three counts corresponding to the solid sphere have a cubic dependency on  $r$ . The relative counts of absentee-voxels corresponding to solid spheres of revolution for radius up to 800 are tabulated in Table 4 and plotted in Figure 9. We observe from these data that with the increasing radius, the value of relative count tends to 0.101 approximately.

The above test results and their theoretical analysis indicate that the ratio of the absentee-voxels

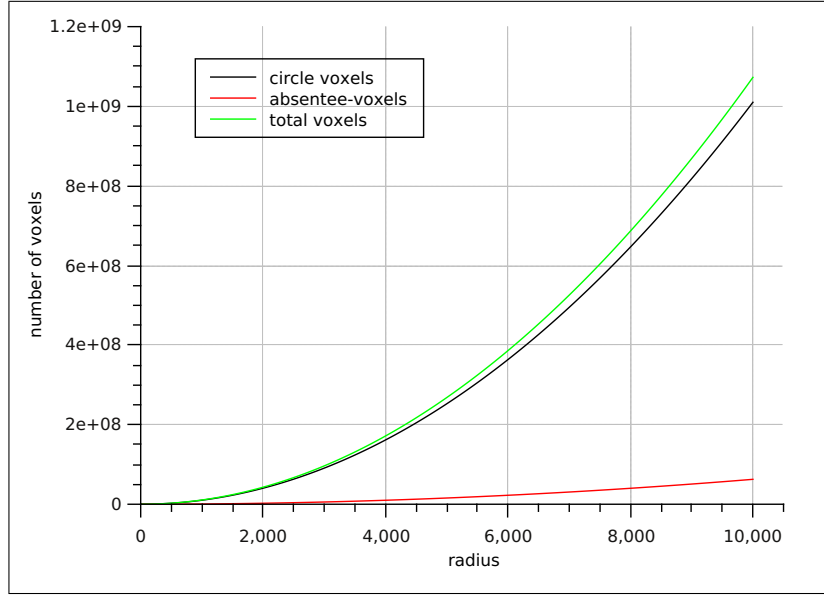


Figure 6: Exact counts of voxels in  $\mathcal{S}_{\mathbb{U}}^{\mathbb{Z}}(r)$ ,  $\mathcal{A}^{\mathbb{Z}^3}(r)$ , and  $\mathcal{S}^{\mathbb{Z}}(r)$ .

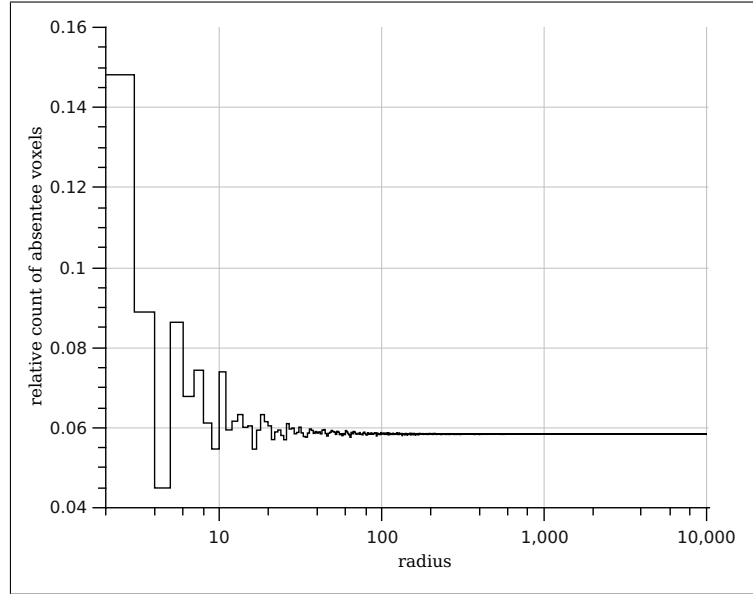


Figure 7: Relative count of absentees versus radius in spheres of revolution.

to the total number of voxels tends to a constant for large radius. The knowledge of geometric distributions of absentee-voxels is shown to be useful for an algorithmic construction of a digital sphere. Although an asymptotic tight bound for the count of absentees has been provided here, the determination of a closed-form solution of the exact count of absentees for a given radius, still remains an open problem. The characterization of these absentees requires further in-depth analysis, especially if we want to generate a solid digital sphere with a set of concentric digital spheres. Apart from spheres, the generation of various other types of surfaces that are devoid of any absentee-voxels, will also have many applications in 3D imaging and graphics, such as the

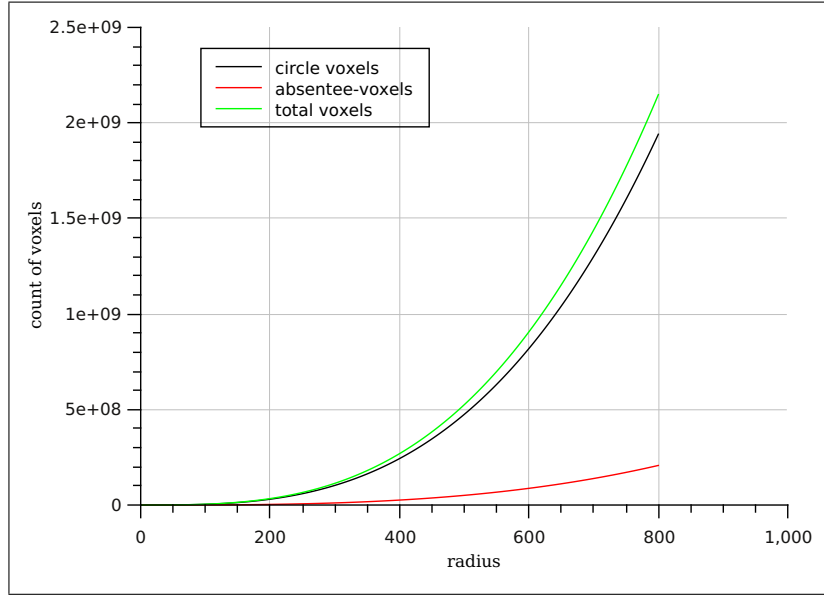


Figure 8: Exact counts of voxels in  $\mathbf{S}_{\mathbb{U}}^{\mathbb{Z}}(r)$  (circle voxels),  $\mathbf{A}^{\mathbb{Z}^3}(r)$  (absentee-voxels), and  $\mathbf{S}^{\mathbb{Z}}(r)$  (total voxels).

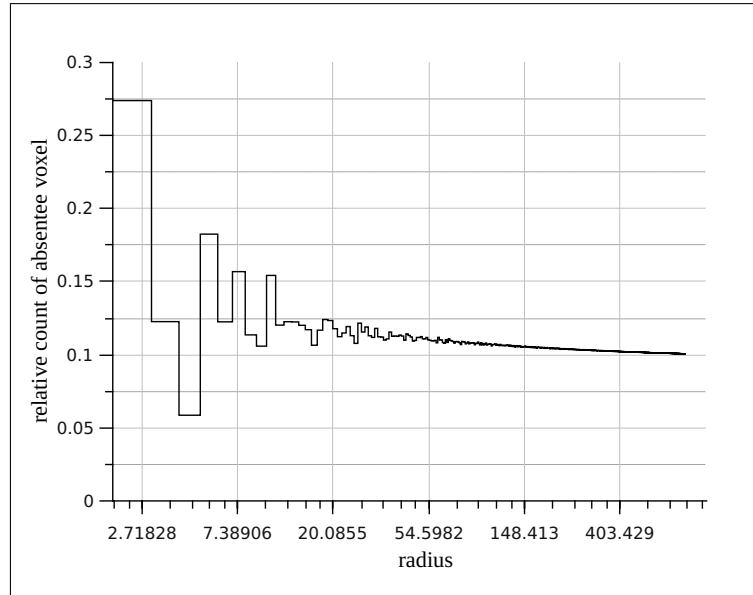


Figure 9: Relative counts of absentee-voxels versus radius in solid spheres of revolution.

Table 2: Relative count of absentees versus radius in spheres of revolution.

$r$	$\alpha_r$	$r$	$\alpha_r$	$r$	$\alpha_r$	$r$	$\alpha_r$
2	0.148148	17	0.059393	180	0.058313	1700	0.058401
3	0.088889	18	0.063269	200	0.058468	1800	0.058382
4	0.044944	19	0.061507	300	0.058389	1900	0.058397
5	0.086331	20	0.060463	400	0.058407	2000	0.058403
6	0.067797	30	0.058811	500	0.058412	2500	0.058386
7	0.074349	40	0.058640	600	0.058353	3000	0.058389
8	0.061162	50	0.059037	700	0.058418	3500	0.058391
9	0.054670	60	0.059276	800	0.058403	4000	0.058393
10	0.073937	70	0.058566	900	0.058390	4500	0.058393
11	0.059435	80	0.058262	1000	0.058401	5000	0.058395
12	0.061617	90	0.058618	1100	0.058381	6000	0.058396
13	0.063277	100	0.058464	1200	0.058404	7000	0.058396
14	0.060094	120	0.058367	1300	0.058405	8000	0.058392
15	0.060453	140	0.058532	1500	0.058399	9000	0.058393
16	0.054637	160	0.058495	1600	0.058387	10000	0.058383

creation of interesting pottery designs, as reported recently [36].

## References

- [1] E. Andres. Discrete circles, rings and spheres. *Computers & Graphics*, 18(5):695–706, 1994.
- [2] E. Andres and M. Jacob. The discrete analytical hyperspheres. *IEEE Trans. Visualization and Computer Graphics*, 3(1):75–86, 1997.
- [3] S. Bera, P. Bhowmick, and B. B. Bhattacharya. A digital-geometric algorithm for generating a complete spherical surface in  $\mathbb{Z}^3$ . In *Proc. International Conference on Applied Algorithms (ICAA'14)*, volume 8321 of *LNCS*, pages 49–61, 2014.
- [4] S. Bera, P. Bhowmick, P. Stelldinger, and B. B. Bhattacharya. On covering a digital disc with concentric circles in  $\mathbb{Z}^2$ . *Theoretical Computer Science*, 506:1–16, 2013.
- [5] P. Bhowmick and B. B. Bhattacharya. Number theoretic interpretation and construction of a digital circle. *Discrete Applied Mathematics*, 156(12):2381–2399, 2008.
- [6] R. Biswas and P. Bhowmick. On finding spherical geodesic paths and circles in  $\mathbb{Z}^3$ . In *Proc. Discrete Geometry for Computer Imagery*, volume 8668 of *LNCS*, pages 396–409. Springer, 2014.
- [7] V. E. Brimkov and R. P. Barneva. Graceful planes and lines. *Theoretical Computer Science*, 283(1):151–170, 2002.
- [8] V. E. Brimkov and R. P. Barneva. On the polyhedral complexity of the integer points in a hyperball. *Theoretical Computer Science*, 406(1-2):24–30, 2008.

Table 3: Exact counts of voxels in  $\mathbf{S}_{\mathbb{U}}^{\mathbb{Z}}(r)$ ,  $\mathbf{A}^{\mathbb{Z}^3}(r)$ , and  $\mathbf{S}^{\mathbb{Z}}(r)$ .

$r$	$ \mathbf{S}_{\mathbb{U}}^{\mathbb{Z}}(r) $	$2 \mathbf{A}^{\mathbb{Z}^3}(r) $	$ \mathbf{S}^{\mathbb{Z}}(r) $	$r$	$ \mathbf{S}_{\mathbb{U}}^{\mathbb{Z}}(r) $	$2 \mathbf{A}^{\mathbb{Z}^3}(r) $	$ \mathbf{S}^{\mathbb{Z}}(r) $
0	1	0	1	80	1941629	233828	2175457
1	7	0	7	90	2761237	333428	3094665
2	53	20	73	100	3785733	452052	4237785
3	143	20	163	150	12749489	1508868	14258357
4	321	20	341	200	30196125	3528744	33724869
5	591	132	723	250	58952525	6810356	65762881
6	945	132	1077	300	101848409	11688640	113537049
7	1483	276	1759	350	161726089	18514264	180240353
8	2153	276	2429	400	241406453	27530128	268936581
9	3039	360	3399	450	343714485	39030584	382745069
10	4121	752	4873	500	471497269	53389448	524886717
20	31377	4192	35569	550	627583253	70890036	698473289
30	104321	13144	117465	600	814799465	91803032	906602497
40	245349	31412	276761	650	1035980249	116498872	1152479121
50	477061	60436	537497	700	1293980265	145396532	1439376797
60	821805	103604	925409	750	1591598569	178467668	1770066237
70	1303165	159636	1462801	800	1931678709	216171360	2147850069

- [9] V. E. Brimkov, R. P. Barneva, B. Brimkov, and F. Vieilleville. Offset approach to defining 3d digital lines. In *Proceedings of the 4th International Symposium on Advances in Visual Computing*, ISVC '08, pages 678–687, Berlin, Heidelberg, 2008. Springer-Verlag.
- [10] V. E. Brimkov, D. Coeurjolly, and R. Klette. Digital planarity — A review. *Discrete Applied Mathematics*, 155(4):468–495, 2007.
- [11] S. E. Cappell and J. L. Shaneson. Some Problems in Number Theory I: The Circle Problem. 2007. <http://arxiv.org/abs/math.NT/0702613>.
- [12] F. Chamizo. Lattice points in bodies of revolution. *Acta Arithmetica*, 85(3):265–277, 1998.
- [13] F. Chamizo and E. Cristobal. The sphere problem and the  $L$ -functions. *Acta Mathematica Hungarica*, 135(1–2):97–115, 2012.
- [14] F. Chamizo, E. Cristóbal, and A. Ubis. Visible lattice points in the sphere. *Journal of Number Theory*, 126(2):200–211, 2007.
- [15] F. Chamizo, E. Cristóbal, and A. Ubis. Lattice points in rational ellipsoids. *Journal of Mathematical Analysis and Applications*, 350(1):283–289, 2009.
- [16] Y. T. Chan and S. M. Thomas. Cramer-Rao lower bounds for estimation of a circular arc center and its radius. *Graphical Models and Image Processing*, 57(6):527–532, 1995.
- [17] T. Christ, D. Pálvölgyi, and M. Stojakovic. Consistent digital line segments. *Discrete & Computational Geometry*, 47(4):691–710, 2012.

Table 4: Relative counts of absentee-voxels versus radius in solid spheres of revolution.

$r$	$\alpha_r$	$r$	$\alpha_r$	$r$	$\alpha_r$	$r$	$\alpha_r$
2	0.27397	16	0.10654	120	0.10654	320	0.10300
3	0.12270	17	0.11685	130	0.10620	340	0.10283
4	0.05865	18	0.12414	140	0.10606	360	0.10250
5	0.18257	19	0.12345	150	0.10582	380	0.10233
6	0.12256	20	0.11786	160	0.10523	400	0.10237
7	0.15691	30	0.11190	170	0.10482	420	0.10219
8	0.11363	40	0.11350	180	0.10482	450	0.10198
9	0.10591	50	0.11244	190	0.10463	500	0.10172
10	0.15432	60	0.11195	200	0.10463	550	0.10149
11	0.12030	70	0.10913	220	0.10403	600	0.10126
12	0.12264	80	0.10748	240	0.10368	650	0.10109
13	0.12249	90	0.10774	260	0.10361	700	0.10101
14	0.12018	100	0.10667	280	0.10328	750	0.10083
15	0.11719	110	0.10661	300	0.10295	800	0.10065

- [18] J. Chun, M. Korman, M. Nöllenburg, and T. Tokuyama. Consistent digital rays. *Discrete & Computational Geometry*, 42(3):359–378, 2009.
- [19] E. R. Davies. A hybrid sequential-parallel approach to accurate circle centre location. *Pattern Recognition Letters*, 7:279–290, 1988.
- [20] M. Doros. On some properties of the generation of discrete circular arcs on a square grid. *Computer Vision, Graphics, and Image Processing*, 28(3):377–383, 1984.
- [21] B. Draine and P. Flatau. Discrete dipole approximation for scattering calculations. *J. Opt. Soc. Am. A*, 11:1491–1499, 1994.
- [22] J. A. Ewell. Counting lattice points on spheres. *The Mathematical Intelligencer*, 22(4):51–53, 2000.
- [23] F. Feschet and J.-P. Reveillès. A Generic Approach for n-Dimensional Digital Lines. In *Proceedings of the 13th international conference on Discrete Geometry for Computer Imagery*, DGCI’06, pages 29–40, Berlin, Heidelberg, 2006. Springer-Verlag.
- [24] C. Fiorio, D. Jamet, and J.-L. Toutant. Discrete circles: an arithmetical approach with non-constant thickness. In A. Y. W. Longin Jean Latecki, David M. Mount, editor, *Vision Geometry XIV, Electronic Imaging, SPIE*, volume 6066, page 60660C, San Jose (CA), USA, 2006.
- [25] C. Fiorio and J.-L. Toutant. Arithmetic discrete hyperspheres and separatingness. In *Proceedings of the 13th international conference on Discrete Geometry for Computer Imagery*, DGCI’06, pages 425–436, Berlin, Heidelberg, 2006. Springer-Verlag.
- [26] J. D. Foley, A. v. Dam, S. K. Feiner, and J. F. Hughes. *Computer Graphics — Principles and Practice*. Addison-Wesley, Reading (Mass.), 1993.

- [27] O. Fomenko. Distribution of lattice points over the four-dimensional sphere. *Journal of Mathematical Sciences*, 110(6):3164–3170, 2002.
- [28] L. Fukshansky, G. Henshaw, P. Liao, M. Prince, X. Sun, and S. Whitehead. On integral well-rounded lattices in the plane. *Discrete & Computational Geometry*, 48(3):735–748, 2012.
- [29] R. M. Haralick. A measure for circularity of digital figures. *IEEE Trans. Sys., Man & Cybern.*, 4:394–396, 1974.
- [30] D. R. Heath-Brown. Lattice points in the sphere. *Number theory in progress. Walter de Gruyter, Berlin*, II:883–892, 1999.
- [31] R. Honsberger. Circles, Squares, and Lattice Points. *Mathematical Gems*, I:117–127, 1973.
- [32] Y. Kenmochi, L. Buzer, A. Sugimoto, and I. Shimizu. Digital planar surface segmentation using local geometric patterns. In *Proceedings of the 14th IAPR international conference on Discrete Geometry for Computer Imagery*, DGCI’08, pages 322–333, Berlin, Heidelberg, 2008. Springer-Verlag.
- [33] R. Klette and A. Rosenfeld. *Digital Geometry: Geometric Methods for Digital Picture Analysis*. Morgan Kaufmann Series in Computer Graphics and Geometric Modeling. Morgan Kaufmann, San Francisco, 2004.
- [34] R. Klette and A. Rosenfeld. Digital straightness: A review. *Discrete Applied Mathematics*, 139(1-3):197–230, 2004.
- [35] M. Kühleitner. On lattice points in rational ellipsoids: An omega estimate for the error term. *Abhandlungen Aus Dem Mathematischen Seminar Der Universitat Hamburg*, 70(1):105–111, 2000.
- [36] G. Kumar, N. Sharma, and P. Bhowmick. Wheel-throwing in digital space using number-theoretic approach. *International Journal of Arts and Technology*, 4(2):196–215, 2011.
- [37] H. Maehara. On a sphere that passes through  $n$  lattice points. *European Journal of Combinatorics*, 31(2):617–621, 2010.
- [38] A. Magyar. On the distribution of lattice points on spheres and level surfaces of polynomials. *Journal of Number Theory*, 122(1):69–83, 2007.
- [39] F. Mignosi. On the number of factors of Sturmian words. *Theoretical Computer Science*, 82(1):71–84, 1991.
- [40] C. Montani and R. Scopigno. Graphics gems (Chapter: *Spheres-to-voxels conversion*), A. S. Glassner (Ed.). pages 327–334. Academic Press Professional, Inc., San Diego, CA, USA, 1990.
- [41] B. Nagy. Characterization of digital circles in triangular grid. *Pattern Recognition Letters*, 25(11):1231–1242, 2004.

- [42] A. Nakamura and K. Aizawa. Digital circles. *Computer Vision, Graphics, and Image Processing*, 26(2):242–255, 1984.
- [43] S. Pal and P. Bhowmick. Determining digital circularity using integer intervals. *Journal of Mathematical Imaging and Vision*, 42(1):1–24, 2012.
- [44] P. Stelldinger. *Image Digitization and its Influence on Shape Properties in Finite Dimensions*. IOS Press, 2007.
- [45] S. M. Thomas and Y. T. Chan. A simple approach for the estimation of circular arc center and its radius. *Computer Vision, Graphics, and Image Processing*, 45(3):362–370, 1989.
- [46] J.-L. Toutant, E. Andres, and T. Roussillon. Digital circles, spheres and hyperspheres: From morphological models to analytical characterizations and topological properties. *Discrete Applied Mathematics*, 161:2662–2677, 2013.
- [47] K.-M. Tsang. Counting lattice points in the sphere. *Bulletin of the London Mathematical Society*, 32:679–688, 2000.
- [48] D.-M. Woo, S.-S. Han, D.-C. Park, and Q.-D. Nguyen. Extraction of 3D Line Segment Using Digital Elevation Data. In *Proceedings of the 2008 Congress on Image and Signal Processing*, volume 2 of *CISP'08*, pages 734–738, Washington, DC, USA, 2008. IEEE Computer Society.
- [49] P. C. Yuen and G. C. Feng. A novel method for parameter estimation of digital arc. *Pattern Recognition Letters*, 17(9):929–938, 1996.
- [50] E. Zubko, D. Petrov, Y. Grynko, Y. Shkuratov, H. Okamoto, K. Muinonen, T. Nousiainen, H. Kimura, T. Yamamoto, and G. Videen. Validity criteria of the discrete dipole approximation. *Applied Optics*, 49(8):1267–1279, 2010.